Research paper

Evaluation of Strontium Ferrite (SrFe₁₂O₁₉) in Ammonium Perchlorate-based Composite Propellant Formulations

Sunil Jain,[1] Dhirendra R. Kshirsagar,[1] Vrushali H. Khire,[1,*] Balasubramanian Kandasubramanian[2]

1) *High Energy Materials Research Laboratory, DRDO, Sutarwadi, Pune 411021, India*
2) *Defence Institute of Advanced Technology, Deemed University, Pune 411025, India*
*E-mail: vruushalikhirrey@gmail.com

Abstract: In the present work, various propellant compositions were prepared by incorporating strontium ferrite ($SrFe_{12}O_{19}$) in an ammonium perchlorate (AP), aluminium powder and hydroxyl-terminated polybutadiene (HTPB) based standard composite propellant. The compositions were then studied by assessing the effect of the $SrFe_{12}O_{19}$ content on the propellant slurry viscosity, and the mechanical and ballistic properties. The results showed that as the percentage of $SrFe_{12}O_{19}$ in the propellant was increased, the end of mix (EOM) slurry viscosity, tensile strength and E-modulus increased, while the elongation decreased. The ballistic properties data revealed that the burning rate of the propellant composition containing 1.0% $SrFe_{12}O_{19}$ was enhanced by around 15% (at 6.86 MPa) compared to the standard composition burning rate.

Keywords: composite propellant, strontium ferrite, pressure exponent, burning rate

Symbols and abbreviations
AP   Ammonium perchlorate, NH_4ClO_4
EOM   End of mixing

HTPB   Hydroxyl-terminated polybutadiene
SSBR   Solid strand burning rate

1   Introduction

Composite propellants are extensively used in defence as well as in satellite launch vehicles. They contain a polymeric fuel/binder (HTPB), an oxidizer (ammonium perchlorate, AP) and a metallic fuel (aluminium powder, Al) supplemented with other minor additives. A composite propellant's burning rate depends mainly on the oxidizer, burning rate modifiers and metallic fuel characteristics. Burning rate modifiers (mainly transition metal oxides and their complexes) are almost invariably used in all high burning rate propellant compositions for various reasons [1-5]. Furthermore, research is being carried out on the development of new types of ballistic modifier for composite propellants [6, 7]. Ferrites are industrially important compounds, consisting of a mixed of oxides of iron and one or more other metals [8, 9]. They have also been studied as possible burning rate modifiers for composite propellants. The catalytic effect of nickel and erbium ferrites on various oxidizers (potassium and sodium chlorates/perchlorates) was studied by Haralambous *et al.* [10] and were found to be effective in enhancing the thermal decomposition of the oxidizers used. Singh *et al.* [11] studied the thermal decomposition of AP catalyzed by mixed ternary ferrite nanocrystallites ($NiZnFe_2O_4$, $CuCoFe_2O_4$, *etc.*). They found the following order for catalytic activity of the mixed ferrites:

$$CoZnFe_2O_4 > CoNiFe_2O_4 > CuZnFe_2O_4 > CuCoFe_2O_4 > NiCuFe_2O_4 > NiZnFe_2O_4 \quad (1)$$

Furthermore, Singh *et al.* [12] studied the effect of binary transition metal ferrite nanocrystals ($CuFe_2O_4$, $CoFe_2O_4$ and $NiFe_2O_4$) on AP thermal decomposition and determined the order of effectiveness as:

$$CoFe_2O_4 > CuFe_2O_4 > NiFe_2O_4 \quad (2)$$

Srivastava *et al.* [13] have worked on the evaluation of nanoferrites in composite propellants and found that $NiCuZnFe_2O_4$was the most effective ferrite in AP thermal decomposition, as well as in enhancing the burning rate of composite propellants. Singh *et al.* [14] also explored the catalytic behaviour of Cd nanocrystals and $CdFe_2O_4$ on composite solid propellants and found $CdFe_2O_4$ to

be better than Cd nanocrystals in increasing the composite propellant's burning rate. Singh *et al.* [15] synthesised and characterized nanoferrites of Mn, Co, Ni in the form of nanorod, nanosphere, and nanocube morphologies. They studied the catalytic effect of these nanoferrites on AP and found the order of effectiveness to be:

$$MnFe_2O_4 > CoFe_2O_4 > NiFe_2O_4 \tag{3}$$

From a literature survey, it became obvious that ferrites are effective catalysts for enhancing the burning rate of composite propellants. However, detailed studies using ferrites in propellant compositions have not so far been carried out.

Strontium ferrite, which has a magnetoplumbite structure with hexagonal symmetry, was chosen for the present study based on the hypothesis that it may also work as a burning rate modifier for composite propellants in a similar manner to the ferrites mentioned. This hypothesis was further supported by the following literature that shows the catalytic effect of strontium ferrite on several types of reactions, including fuel combustion. Bukhtiyarova *et al.* [16] investigated the catalytic combustion of methane on substituted strontium ferrite and found it was effective. Ji *et al.* [17] prepared porous strontium ferrite and evaluated its catalytic effectiveness for the combustion of toluene. Aziz *et al.* [18] studied solar photoactivity of strontium ferrite nanocomposite photocatalyst supported on titania. Sheshko *et al.* [19] carried out catalytic hydrogenation of carbon monoxide over nanostructured perovskite-like gadolinium and strontium ferrite. Liu *et. al.* [20] found strontium ferrite was effective in the microwave-induced catalytic application for the degradation of organic dyes. Shaula *et al.* [21] studied its application as a catalytic component (three-way) for car exhaust pollution control.

In the present paper, the characterization of strontium ferrite (SrFe$_{12}$O$_{19}$) and its effect on various composite propellant properties is presented in detail.

2   Experimental

2.1 Materials

Bimodal AP (300 μm and 50 μm) was used in the composite propellant formulations studied. The 300 μm AP (average size) was received from M/s Pandian Chemicals Ltd., Cuddalore (India). A pin disc mill (ACM-10) was used to prepare 50 μm AP by grinding 300 μm AP. HTPB, having an average molecular weight of 2560 and hydroxyl number 41.8 mg KOH/g,

was purchased from M/s Anabond Ltd., Chennai (India) and used without any processing. Aluminium powder (15 μm average particle size) was purchased from M/s The Metal Powder Company, Madurai (India) and also employed as received. $SrFe_{12}O_{19}$, toluene di-isocyanate (TDI), dioctyladipate (DOA), 1,4-butanediol (n-BD), trimethylolpropane (TMP) and *N*-phenyl-2-naphthylamine (antioxidant) were purchased on the open market and utilized without any processing.

2.2 Characterization

Material and phase identification analysis of $SrFe_{12}O_{19}$ was performed on a Phillips PANalyticalX'pert pro powder X-ray diffractometer using Cu-K$_\alpha$ radiation. A laser diffraction-based particle size analyser CILAS (model 1064L) was employed to analyse the average particle size of $SrFe_{12}O_{19}$ in the wet mode. The morphology of the $SrFe_{12}O_{19}$ particles was investigated employing a Zeiss Sigma Field Emission Scanning Electron Microscope (FESEM) having a resolution capability of 1.4 nm. A BET surface area analyser, Micromeritics (Gemini VII 2390t), was employed to analyse the specific surface area of $SrFe_{12}O_{19}$. The propellant slurry EOM viscosity was determined with a Brookfield dial viscometer (model HBT). A Hounsfield universal testing machine (UTM) was used to evaluate the cured propellant's mechanical properties (tensile strength, E-modulus and percentage elongation) at a strain rate of 50 mm/min. A gas pycnometer was used to measure the density of AP, strontium ferrite and propellant samples. A Bundesanstalt fur Materialprufung (BAM) fall hammer instrument, OZM make (model No. BFH-10) with 2 kg drop weight, was used to study the impact sensitivity of the propellant compositions [22]. A BAM friction instrument (model No. FSKM-10) was used to study the friction sensitivity of the propellant compositions [23]. A laser flash method based instrument (Flashline-3000) of Anter Corporation, USA, was used to measure the thermal transport properties (conductivity, specific heat, *etc.*) of the studied propellants. A differential scanning calorimeter (DSC) of TA Instruments (model Q20) was utilized to perform the thermal decomposition study (at 10 °C/min heating rate). The calorimetric values (*cal-val*) of the propellant samples were measured employing a Parr isoperibol calorimeter (model 6200) under an N_2 atmosphere [24]. The acoustic emission technique was used to measure the solid strand burning rate (SSBR) of the studied propellants, employing an N_2 pressurized metal bomb. Compatibility studies were carried out on a vacuum stability tester (VST) of OZM (model STABIL) at 100 °C for 40 h.

2.3 Preparation of composite propellants

Mixing of the propellant compositions was performed in a 15 L vertical planetary mixer following set procedures [25]. The sequence of addition was as follows (with mixing after each incremental addition): binder (excluding TDI), antioxidant, catalyst, aluminium powder, AP (50 μm) and AP (300 μm). Maintaining the mix temperature at 40 ±2 °C, mixing of the composition was continued for 30 min under vacuum, and then TDI was added and mixing was continued for a further 40 min. The resultant propellant slurry was cast by the vacuum casting technique into a mould (100 mm inner diameter) and the mould was then kept in a water-jacketed oven for propellant curing for 5 days at 50 °C.

Table 1 lists the composition details of all the propellant formulations prepared in the course of this study. By incorporating 0.25%, 0.50%, 0.75% and 1.0% of SrFe$_{12}$O$_{19}$ into the standard propellant composition, four propellant compositions were processed. Two further propellant compositions were processed with 16% and 14% aluminium powder, both containing 0.5% SrFe$_{12}$O$_{19}$.

Table 1.   Propellant formulations

Ingredients	Composition [wt.%]						
	Standard	1	2	3	4	5	6
Binder (HTPB+TDI+DOA)	14.00	14.00	14.00	14.00	14.00	14.00	14.00
AP Coarse (300 μm)	52.50	52.25	52.00	51.75	51.50	54.00	56.00
AP Fine (50 μm)	15.50	15.50	15.50	15.50	15.50	15.50	15.50
Aluminium powder (15 μm)	18.00	18.00	18.00	18.00	18.00	16.00	14.00
Strontium ferrite (SrFe$_{12}$O$_{19}$)	–	0.25	0.50	0.75	1.00	0.50	0.50

3   Results and Discussion

3.1 SrFe$_{12}$O$_{19}$ characterization

SrFe$_{12}$O$_{19}$ was characterized prior to its incorporation in the propellant formulations. Table 2 lists the thermo-physical properties of SrFe$_{12}$O$_{19}$ from the characterization carried out in this study, from the manufacturer of the powder and also from the literature [26].

A material and phase identification analysis of SrFe$_{12}$O$_{19}$ was performed on an XRD instrument at a scanning rate of 2°/min. The resultant XRD pattern

obtained is shown in Figure 1. It has around 15 sharp peaks corresponding to different 2θ values and clearly reveals the crystalline nature of $SrFe_{12}O_{19}$. The XRD peaks obtained match closely the standard XRD pattern of strontium ferrite (JCPDS Card No. 84-1531).

Table 2. Thermo-physical properties of strontium ferrite

Property	Values as *per* the available literature	Values given by the manufacturer	Characteri-zed value
Density [g/cm^3]	5.18	–	5.15[a]
Melting point [°C]	>450	–	>350[b]
Particle size [μm]	–	<45 (325 mesh)	2.5
Specific surface area [m^2/g]	–	–	0.6
Assay [%]	–	99.5	–
Thermal conductivity [W/m·K]	2.9	–	–
Coefficient of thermal expansion [cm/cm·K]	Parallel: 14×10^{-6} Perpendicular: 10×10^{-6}	–	–
Modulus of elasticity [Pa]	18×10^{11}	–	–

[a] by Gas Pycnometer; [b] by Melting Point apparatus.
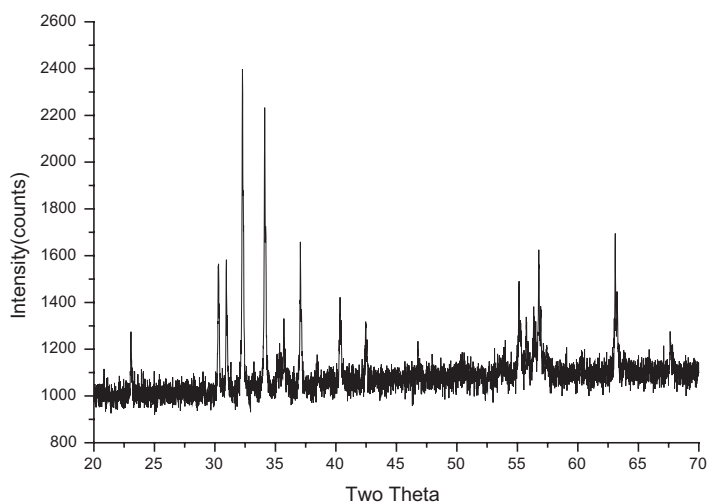
Figure 1. X-ray diffraction patterns of strontium ferrite

A laser diffraction-based analyser CILAS (1064L) was used to analyse the particle size of SrFe$_{12}$O$_{19}$. The average particle size (surface mean diameter) of the powder was around 2.5 µm. The finer catalyst particles are desirable as it disperses homogeneously throughout the propellant matrix and also provides a large surface area for catalytic reactions.

FESEM was used to analyse the surface morphology of SrFe$_{12}$O$_{19}$. The image (Figure 2) infers that the particles of SrFe$_{12}$O$_{19}$ are irregular in shape and non-agglomerated. Furthermore, the size of the particles as seen from this image fell in the range of 1-8 µm.

A BET specific surface area analyser was used to analyse the specific surface area of SrFe$_{12}$O$_{19}$ using N$_2$. The measured specific surface area of SrFe$_{12}$O$_{19}$ was around 0.6 m^2/g. A high specific surface area of the catalyst is desirable as it provides a large number of active sites for catalytic reactions.
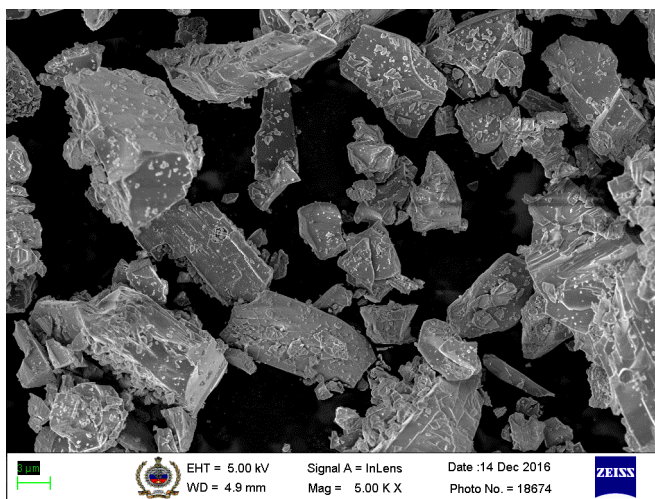
Figure 2.   Field emission – scanning electron microscopic image of strontium ferrite

3.2 Ground AP (50 µm) characterization

The procured 300 µm AP was used to prepare 50 µm AP by grinding using a pin disc mill (ACM-10). The ground AP particle size was determined by employing the sieve analysis method using 150 and 200 No. British Standard (B.S.) test sieves and following the standard procedure [27]. The size distribution of the ground AP particles is presented in Table 3.

Table 3.   Particle size distribution of ground AP (50 µm)

B.S. Sieve No. (opening size)	% of retained particles on the sieve	Average particle size [µm]
150 (105 µm)	6.05	
200 (75 µm)	14.25	50.43
Pan (0 µm)	79.70	

3.3 Evaluation of $SrFe_{12}O_{19}$ in composite propellants

3.3.1 Viscosity, mechanical properties and density

The EOM viscosity, mechanical properties and density data of the compositions are listed in Table 4. The EOM viscosity data indicated that as the overall average particle size of the fillers was decreased (by adding finer $SrFe_{12}O_{19}$ or aluminium powder in place of coarser AP), the EOM of the propellant compositions increased.

Table 4.   Effect of strontium ferrite on viscosity, mechanical properties and density of the composite propellant

Composition	Viscosity at 40 °C [Pa·s]	Tensile strength [MPa]	E-Modulus [MPa]	Elongation [%]	Density [kg/m³]
Standard	670	0.62	3.43	45.00	1777
1	736	0.65	3.75	39.58	1777
2	800	0.76	4.15	38.53	1783
3	832	0.78	4.30	34.68	1790
4	832	0.79	4.43	34.82	1794
5	752	0.62	2.68	40.67	1777
6	662	0.55	2.65	38.61	1760

The data on the mechanical properties (Table 4) infer that as the percentage of $SrFe_{12}O_{19}$ in a propellant composition (comp. 1-4) was increased, the tensile strength and E-modulus increased, although the elongation decreased, which is probably due to the enhancement of the dewetting strain of the propellant on addition of fine $SrFe_{12}O_{19}$ in place of coarse AP particles in the propellant compositions. It is mentioned in the literature [28, 29] that when samples of filled polymer systems are subjected to a stress, a polymer system filled with coarse particles starts dewetting at a lower stress compared to a system containing fine particles. The dewetting of binder from particles involves the formation of vacuoles. The vacuoles will form at coarse particles in a binder

at a lower elongation than at fine particles under the same loading conditions. Thus, the tensile strength increases as the fine particle content in the composite material increases.

    The data on propellant density (Table 4) infer that as the percentage of SrFe$_{12}$O$_{19}$ in a composition was increased, its density also increased. This may be because of replacement of low density AP with higher density SrFe$_{12}$O$_{19}$ and/or enhanced packing of the propellant's powder ingredients due to the incorporation of fine SrFe$_{12}$O$_{19}$ particles.

3.3.2 Propellant sensitivity

Table 5 lists the measured impact and friction sensitivity values for the standard composition and the compositions containing 0.25% SrFe$_{12}$O$_{19}$ (comp. 1) and 1% SrFe$_{12}$O$_{19}$ (comp. 4). The impact height corresponding to 50% probability of a decomposition/explosion was taken as representative of impact sensitivity. The maximum load which did not result in any decomposition/explosion for six consecutive experiments was taken as a measure of the friction sensitivity of that composition. The results in Table 5 revealed that the compositions containing SrFe$_{12}$O$_{19}$ show minor increases in both impact and friction sensitivity values compared to the values obtained for the standard composition. These increases in sensitivity values may be attributed to enhanced thermal decomposition of the propellant by SrFe$_{12}$O$_{19}$ [30].

Table 5.   Effect of strontium ferrite on the sensitivity of the propellants

Composition	Impact sensitivity ($H_{50\%}$) [cm]	Friction sensitivity [N]
Standard	52.5	128
1	50	96
4	45	72

    Furthermore, the differences between the friction sensitivity values of strontium ferrite based propellant compositions and the standard propellant composition were higher than the differences in the impact sensitivity values. It is also reported in the literature that for some burning rate modifiers, the impact value is not much affected by the presence of burning rate modifiers, but friction sensitivity values are affected significantly by the burning rate modifiers [30].

3.3.3 Thermal transport properties

The thermal conductivity, diffusivity and specific heat of the propellant compositions were evaluated using a thermal apparatus based on flash laser [31, 32]. Table 6 lists data obtained for the standard as well as for the compositions

containing 0.25% $SrFe_{12}O_{19}$ (comp. 1) and 1% $SrFe_{12}O_{19}$ (comp. 4). These reveal that the thermal transport properties of the propellant are changed marginally by the addition of $SrFe_{12}O_{19}$ (partly replacing AP) in the standard propellant composition. The thermal conductivity values of $SrFe_{12}O_{19}$ and AP are 2.9 W/m·K and 0.403 W/m·K, respectively. Addition of 1% $SrFe_{12}O_{19}$ (in place of 1% AP) would have resulted in a 5% increase in thermal conductivity of the propellant, however, due to experimental errors, this was not reflected in the results [32].

Table 6.   Effect of strontium ferrite on the thermal transport properties of composite propellant formulations

Composition	Thermal conductivity [W/m·K]	Thermal diffusivity [cm²/s]	Specific heat [J/kg·K]
Standard	0.49	0.0030	929.4
1	0.47	0.0034	792.2
4	0.49	0.0035	776.3

3.3.4 Thermal decomposition of the propellants

The standard composition and the propellant compositions containing $SrFe_{12}O_{19}$ were studied for their thermal decomposition behaviour employing DSC. Table 7 lists the peak temperature values of the endotherms and exotherms obtained during thermal analysis of the propellant compositions. The standard composition showed an endotherm at around 242 °C, attributed to a phase change (orthorhombic to cubic) of AP. A minor exothermic decomposition peak was observed at around 292 °C, mainly due to incomplete decomposition of AP. On further heating, a sharp exothermic decomposition peak (II exotherm) was observed at around 394 °C. This II exotherm is the peak which is affected significantly by the presence of $SrFe_{12}O_{19}$. As the percentage of $SrFe_{12}O_{19}$ in the propellant composition was increased from 0.25% to 1.0%, the II exothermic peak shifted to lower temperatures, as reported in Table 7. Thus, the thermal analysis infers that $SrFe_{12}O_{19}$ catalyses significantly the propellant decomposition.

Table 7.   Effect of strontium ferrite on the thermal decomposition temperature of composite propellant formulations

Composition	Endotherm [°C]	Exotherm [°C]	
		I	II
Standard	242	292	394
1	242	285	371
4	243	284	356

3.3.5 Ballistic properties

Table 8 lists the calorimetric values (*cal-val*) of the SrFe$_{12}$O$_{19}$ based propellant compositions, along with the standard composition. The *cal-val* of the standard propellant was 1550 cal/g, whereas on the incorporation of SrFe$_{12}$O$_{19}$, it was reduced marginally. The reduction in *cal-val* may be due to the partial replacement of energetic AP by inert SrFe$_{12}$O$_{19}$. Furthermore, for the compositions containing a lower Al content (comp. 5 and 6) having a constant 0.5% SrFe$_{12}$O$_{19}$, the *cal-val* was reduced compared to the *cal-val* of comp. 2 (18% Al) since the energy of the propellant was decreased by the decrease in Al content.

The solid strand burning rate (SSBR) of the prepared propellant compositions was measured employing the acoustic emission technique [33] in an N$_2$ atmosphere at different pressures and temperatures and the data obtained are listed in Tables 8 and 9.

Table 8.   Ballistic properties at 27 °C of the studied compositions at different pressures

Composition	SSBR in [mm/s] at pressure [MPa]					Pressure exponent (*n*-value)	*cal-val* [cal/g]
	3.92	5.88	6.86	7.84	8.82		
Standard	4.88	6.00	6.11	6.55	6.84	0.41	1550
1	5.19	6.40	6.86	7.05	7.32	0.43	1550
2	5.35	6.46	7.05	7.38	7.52	0.44	1528
3	5.39	6.42	7.09	7.35	7.64	0.44	1525
4	5.57	6.55	7.05	7.43	7.68	0.41	1497
5	6.06	7.15	7.63	8.25	8.46	0.42	1487
6	6.17	7.29	7.82	8.19	8.71	0.42	1484

Table 9.   Ballistic properties at 6.86 MPa of the studied compositions at different temperatures

Composition	SSBR at 6.86 MPa in [mm/s] at temperature [°C]		
	5	27	55
Standard	5.93	6.11	6.45
1	6.35	6.86	6.93
4	6.72	7.05	7.33

Table 8 gives the burning rate data of the studied propellant compositions at different pressures (3.92 MPa to 8.82 MPa) measured at an initial propellant temperature of 27 °C. The results infer that as the percentage of SrFe$_{12}$O$_{19}$ in the propellant was increased at a constant Al content, the burning rate increased

by 0.5%, then remained more or less constant; therefore concentrations beyond 1% $SrFe_{12}O_{19}$ level were not studied. Table 8 also shows a 15% enhancement in the burning rate of the propellant composition having 1.0% $SrFe_{12}O_{19}$ in comparison to the standard composition at 6.86 MPa. The SSBR of the compositions is enhanced with a decrease in Al content at a constant $SrFe_{12}O_{19}$ content (0.5%), as seen in the burning rate data for comp. 2, 5 and 6. This behaviour is due to the fact that Al particles burn away from the propellant burning surface and transfer little heat to the regressing surfaces. A reduction in the Al content increases the AP content, which increases the burning rate.

In spite of the presence of a good percentage of iron in the $SrFe_{12}O_{19}$ compound, not much enhancement in the burning rate was observed in $SrFe_{12}O_{19}$ based composite propellant formulations. The results obtained may be broadly compared with the results obtained by Babu *et al.* [34] on a composite propellant having 86% solid loading. They employed 1.8 μm sized iron oxide, having a surface area of 28.42 m^2/g, in the propellant and reported a 43% increase in burning rate over the standard composition, at 4.22 MPa pressure, with 0.6% catalyst.

Furthermore, the pressure exponent (*n*-value) of the propellant compositions was calculated using the burning rate at several pressures and the results obtained are listed in Table 8. The pressure exponent value of the standard composition was 0.41. This changed marginally upon incorporation of $SrFe_{12}O_{19}$ in the standard composition.

In order to ascertain the effect of the initial propellant temperature on the burning rate, this was measured at different initial temperatures at 6.86 MPa. Table 9 lists the burning rate data at 5 °C, 27 °C and 55 °C initial temperatures and at 6.86 MPa pressure. As expected, all of the compositions showed an increase in burning rate as the initial propellant temperature was increased.

Combustion of a composite propellant is a complex phenomenon. At present, the catalyzed composite propellant combustion mechanism is not clearly understood. However, a few theories have been postulated [35, 36] to understand how catalysts affect the combustion of a composite propellant. In the case of a composite propellant catalyzed by Fe_2O_3, Ni_2O_3, Co_2O_3, *etc.*, the most acceptable mechanism is the enhancement of electron transfer activity through the redox cycle, due to the variable valence nature of these oxides. For strontium ferrite, which contains two metallic elements (strontium and iron), the catalytic mechanism is very difficult to predict. However, the above-mentioned mechanism involving iron oxide may be the one most applicable in strontium ferrite catalyzed composite propellant combustion. In addition, there may be lattice defects in the $SrFe_{12}O_{19}$ in comparison to Fe_2O_3, which probably creates positive holes

and electrons (owing to strontium being beside iron) in the lattice structure. In the decomposition process of AP in the propellant, $SrFe_{12}O_{19}$ may form a bridge for transferring an electron from the ClO_4^- ion to the NH_4^+ ion.

3.3.6 Analysis of propellant combustion residues

To understand the catalytic behaviour of $SrFe_{12}O_{19}$ in composite propellant combustion, the standard propellant sample as well as the propellant samples containing $SrFe_{12}O_{19}$ were subjected to combustion residue analysis. The residue was collected from the bomb calorimeter after burning the propellant sample and was analyzed for the presence of crystalline phases using XRD. The resultant XRD patterns of the analyzed samples are shown in Figure 3. Table 10 lists the chemical compounds predominantly present in the residues and their XRD peak positions. These were obtained by matching the XRDs of the propellant combustion residues (Figure 3) with the standard XRD library using Xpert HighScore XRD software.

Table 10. XRD peaks of the ash from composite propellants

Compo-sition	Compound	ICDD PDF No.	Peak Bragg angle, 2θ (degree)
Standard	Al_2O_3	00-001-1307	31, 33, 35, 37, 39, 42, 46, 47, 48, 51, 58, 61, 62, 65, 67, 74, 77, 82, 86
2	Al_2O_3	00-001-1307	31, 33, 35, 37, 39, 42, 46, 47, 48, 51, 58, 61, 62, 65, 67, 74, 77, 82, 86
	Al_2O_3	00-001-1303	38, 40, 46, 49, 61, 67, 84
	Strontium oxide	01-073-1740	27, 28, 35, 45, 49, 51, 59, 60, 68, 74, 76, 79, 82, 86
	Strontium iron oxide	00-022-1429	32, 33, 42, 43, 45, 47, 57, 58, 66
	Iron oxide (Fe_2O_3)	01-073-0603	35
4	Al_2O_3	00-001-1307	31, 33, 35, 37, 39, 42, 46, 47, 48, 51, 58, 61, 62, 65, 67, 74, 77, 82, 86
	Al_2O_3	01-079-1557	38, 40, 46, 50, 60, 67, 71, 79, 85, 88
	Strontium oxide	01-073-1740	27, 28, 35, 45, 49, 51, 59, 60, 68, 74, 76, 79, 82, 86
	Iron oxide (Fe_2O_3)	01-073-0603	35
	Strontium iron oxide	00-022-1429	32, 33, 42, 43, 45, 47, 57, 58, 66
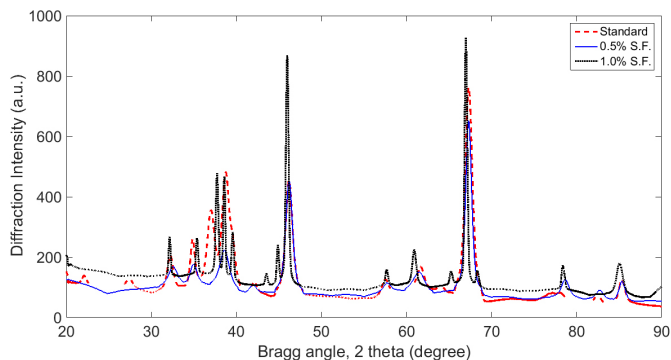
Figure 3. XRD of the ash from the compositions: standard (dashed, red), 2 (solid, blue) and 4 (dotted, black)

The XRD peaks obtained from the residue of the standard propellant only matches predominantly with aluminium oxide. However, the residues of propellant compositions containing $SrFe_{12}O_{19}$ (comp. 2 and 4) show the presence of strontium oxide, strontium iron oxide, iron oxide, *etc.* compounds in addition to aluminium oxide, as is evident from the small peaks at various Bragg angles, shown in Figure 3 and listed in Table 10. The presence of various compounds other than the initial $SrFe_{12}O_{19}$ in the ash, confirms that $SrFe_{12}O_{19}$ has taken part in the chemical reactions during propellant combustion.

3.3.7 Compatibility study of strontium ferrite based propellant formulations

The compatibility of strontium ferrite with other composite propellant ingredients was studied using a vacuum stability tester (VST). The standard composite propellant and the propellant based on strontium ferrite (comp. 4) were heated separately under vacuum at 100 °C for 40 h in glass test tubes and the gas evolved by each sample was measured. The volume of gas evolved from the standard composite propellant and the propellant based on strontium ferrite (comp. 4) was 0.093 cm^3/g and 0.113 cm^3/g, respectively. The above results show that $SrFe_{12}O_{19}$ is compatible with all of the other raw materials of the standard propellant composition, since the evolved gas is comparable in both cases and also well below the 2 cm^3/g limit for incompatibility, as *per* MIL-STD-286C [37, 38].

4   Conclusions

Strontium ferrite was incorporated in an 86% solid loading composite propellant formulation. The EOM viscosity of the standard composition propellant slurry was 670 Pa·s, which upon incorporation of SrFe$_{12}$O$_{19}$ from 0.25% to 1.0% level, increased from 736 Pa·s to 832 Pa·s. The tensile strength and E-modulus increased for the propellant containing 1% SrFe$_{12}$O$_{19}$ compared to the standard composition, however the elongation decreased. The propellant friction and impact sensitivity data demonstrated that SrFe$_{12}$O$_{19}$ causes a minor increase in sensitivity of the propellant compositions. The burning rate data revealed that there was ~15% enhancement in SSBR with 1% SrFe$_{12}$O$_{19}$ at 6.86 MPa in comparison to the standard composition, with a slight change in the pressure exponent values.

References

[1] Kishore, K.; Sunitha, M.R. Mechanism of Catalytic Activity of Transition Metal Oxide on Solid Propellant Burning Rate. *Combust. Flame* **1978**, *33*: 311-314.

[2] Komarov, V.F. Catalysis and Inhibition of the Combustion of Ammonium Perchlorate Based Solid Propellants. *Combust. Explos. Shock Waves* **1999**, *35*(6): 670-683.

[3] Stephens, M.A.; Petersen, E.L.; Reid, D.L.; Carro, R.; Seal, S. Nano Additives and Plateau Burning Rates of Ammonium Perchlorate-based Composite Solid Propellants. *J. Propul. Power.* **2009**, *25*(5): 1068-1078.

[4] Nguyen, T.T. *The Effects of Ferrocenic and Carborane Derivatives Burn Rate Catalyst in AP Composite Propellant Combustion: Mechanism of Ferrocene-Catalysed Combustion.* DSTO-TR-0121, DSTO, **1995**.

[5] Gore, G.M.; Tipare, K.R.; Bhatewara, R.G.; Prasad, U.S.; Gupta, M.; Mane, S.R. Evaluation of Ferrocene Derivatives as Burn Rate Modifiers in AP/HTPB-based Composite Propellants. *Def. Sci. J.* **1999**, *49*(2): 151-158.

[6] Talawar, M.B.; Divekar, C.N.; Makashir, P.S.; Asthana, S.N. Tetrakis-(4-Amino-1,2,4-Triazole) Copper Perchlorate: A Novel Ballistic Modifier for Composite Propellants. *J. Propul. Power* **2005**, *21*(1): 186-189.

[7] Nair, J.K.; Talawar, M.B.; Mukundan, T. Transition Metal Salts of 2,4,6-Trinitroanilinobenzoic Acid - Potential Energetic Ballistic Modifiers for Propellants. *J. Energ. Mater*. **2001**, *19*(2-3): 155-162.

[8] Verma, A.; Pandey, O.P.; Sharma, P. Strontium Ferrite Permanent Magnet. An Overview. *Indian J. Eng. Mater. Sci.* **2000**, 7: 364-369.

[9] Valenzuela, R. Novel Applications of Ferrites, *Physics Research International* **2012**, Article ID 591839; DOI: 10.1155/2012/591839.

[10] Haralambous, K.J.; Loizos, Z.; Spyrellis, N. Catalytic Properties of some Mixed Transition-Metal Oxides. *Mater. Lett.* **1991**, *11*(3-4): 133-141.

[11] Singh, G.; Kapoor, I.P.S.; Dubey, S.; Siril, P.F., Jian, Y.; Zhao, F.Q., Rong-Zu, H.U. Effect of Mixed Ternary Transition Metal Ferrites Nanocrystallites on the Thermal Decomposition of Ammonium Perchlorates. *Thermochim. Acta*. **2008**, 477: 42-47.

[12] Singh, G.; Kapoor, I.P.S.; Dubey, S.; Siril, P.F. Kinetics of Thermal Decomposition of Ammonium Perchlorate with Nanocrystals of Binary Transition Metal Ferrites. *Propellants Explos. Pyrotech.* **2009**, *34*: 72-77.

[13] Srivastava, P.; Kapoor, I.P.S.; Singh, G. Nanoferrites: Preparation, Characterization and Catalytic Activity. *J. Alloys Compd.* **2009**, *485*(1-2): 88-92.

[14] Singh, G.; Kapoor, I.P.S.; Dubey, R.; Srivastava, P. Preparation, Characterization and Catalytic Behaviour of $CdFe_2O_4$ and Cd Nanocrystals on AP, HTPB and Composite Solid Propellants. Part 79. *Thermochimic. Acta* **2010**, *511*(1-2): 112-118.

[15] Singh, S.; Srivastava, P.; Singh, G. Nanorods, Nanospheres, Nanocubes: Synthesis, Characterization and Catalytic Activity of Nanoferrites of Mn, Co, Ni. Part 89. *Mater. Res. Bull.* **2013**, *48*(2): 739-746.

[16] Bukhtiyarova, M.V.; Ivanova, A.S.; Slavinskaya, E.M.; Plyasova, L.M.; Rogov, V.A.; Kaichev, V.V.; Noskov, A.S. Catalytic Combustion of Methane on Substituted Strontium Ferrite. *Fuel* **2011**, 90: 1245-1256.

[17] Ji, K.; Dai, H.; Deng, J.; Zhang, L.; Jiang, H.; Xie, S.; Han, W. One Pot Hydrothermal Preparation and Catalytic Performance of Porous Strontium Ferrite Hollow Spheres for the Combustion of Toluene. *J. Mol. Catal.* A *Chem.* **2013**, 370: 189-196.

[18] Aziz, A.A.; Puma, G.L.; Ibrahim, S.; Saravanan, P. Preparation, Characterization and Solar Photoactivity of Titania Supported Strontium Ferrite Nanocomposite Photocatalyst. *J. Exp. Nanosci.* **2013**, *8*(3): 295-310.

[19] Sheshko, T.F.; Serov, Y.M.; Dement'eva, M.V.; Shul'ga, A.; Chislova, I.V.; Zvereva, I.A. Catalytic Hydrogenation of Carbon Monoxide over Nanostructured Perovskite-like Gadolinium and Strontium Ferrite. *Russ. J. Phys. Chem. A* **2016**, *90*(5): 926-931.

[20] Liu, X.; Zhang, T.; Zhang, L. Microwave Induced Catalytic Application of Magnetically Separable Strontium Ferrite in the Degradation of Organic Dyes: Insight into the Catalytic Mechanism. *Sep. Purif. Technol.* **2018**, 195:192-198.

[21] Shaula, A.L.; Karavai, O.V.; Ivanova, Y.A.; Mikhalev, S.M.; Tarelho, L.A.C. Strontium Ferrite as a Three-Way Catalyst Component. *Mater. Lett.* **2018**, 216: 273-276

[22] *Explosives, Impact Sensitivity Tests.* STANAG No. 4489, 1st ed., September 17, **1999**.

[23] *Explosives, Friction Sensitivity Tests.* STANAG No. 4487, 1st ed., August 22, **2002**.

[24] Jawale, L.S.; Dey, C.; Mehilal; Gupta, M.; Bhattacharya, B. Effect of Experiment Environment on Calorimetric Value of Composite Solid Propellants. *Def. Sci. J.* **2013**, *63*(5): 467-472.

[25] Muthiah, R.; Manjari, R.; Krishnamurthy, V.N. Rheology of HTPB Propellant: Effect of Mixing Speed and Mixing Time. *Def. Sci. J.* **1993**, *43*(2): 167-172

[26] *Standard Specifications for Permanent Magnet Materials*. MMPA Standard No. 0100-00, Magnetic Materials Producers Association, Chicago, USA, **2000**.

[27] Dodds, J. Techniques to Analyse Particle Size of Food Powders. In: *Handbook of Food Powders*, *Processes and Properties* (Bhandari, B.; Bansal, N.; Zhang, M.; Schuck, P., Eds.), Woodhead Publishing, Oxford, **2013**, pp. 309-338; ISBN 978-0-85709-513-518.

[28] Gocmez, A.; Erisken, C.; Yilmazer, U.; Pekel, F.; Ozkar, S. Mechanical and Burning Properties of Highly Loaded Composite Propellants. *J. Appl. Polym. Sci.* **1998**, *67*: 1457-1464.

[29] Jones, H.C.; Yiengst, H.A. Dilatometer Studies of Pigment-Rubber Systems. *Ind. Eng. Chem.* **1940**: 1354-1359.

[30] Bazaki, H.; Kubota, N. Friction Sensitivity Mechanism of Ammonium Perchlorate Composite Propellants. *Propellants Explos. Pyrotech.* **1991**, *16*: 43-47.

[31] Chiguma, J.; Johnson, E.; Shah P.; Gornopolskaya, N.; Jones, W. Thermal Diffusivity and Thermal Conductivity of Epoxy-Based Nanocomposites by the Laser Flash and Differential Scanning Calorimetry Techniques. *OJCM* **2013**, 3: 51-62.

[32] Kalal, R.K.; Ropia, B.; Bansode, M.K.; Shekhar, H.; Rao, C.G. Measurement of Direction Dependent Thermal Properties of Graphite-1346. *AIP Conf., Proc. Sem., 1536*, **2013**, 1352-1354.

[33] Gupta, G.; Jawale, L.; Mehilal; Bhattacharya, B. Various Methods for the Determination of the Burning Rates of Solid Propellants – An Overview. *Cent. Eur. J. Energ. Mater.* **2015**, *12*(3): 593-620.

[34] Babu, S.K.V.; Raju, P.K.; Thomas, C.R.; Hamed, S.A.; Ninan, K.N. Studies on Composite Solid Propellant with Tri-Modal Ammonium Perchlorate Containing an Ultrafine Fraction. *Def. Tech.* **2017**, 13: 239-245.

[35] Kishore, K.; Sunitha, M.R. Mechanism of Catalytic Activity of Transition Metal Oxides on Solid Propellant Burning Rate. *Combust. Flame* **1978**, *33*: 311-314.

[36] Komarov, V.F. Catalysis and Inhibition of the Combustion of Ammonium Perchlorate Based Solid Propellants. *Combust. Explos. Shock Waves* **1999**, *35*(6): 670-683.

[37] *Propellants, Solid Sampling, Examination and Testing*. MIL-STD-286C: Method 403.1.3, **1991**.

[38] Kurva, R.; Gupta, G.; Dhabbe, K.I.; Jawale, L.S.; Kulkarni, P.S.; Maurya, M. Evaluation of 4-(Dimethylsilyl) Butyl Ferrocene Grafted HTPB as a Burning Rate Modifier in Composite Propellant Formulation using Bicurative System. *Propellants Explos. Pyrotech.* **2017**, *42*(4): 401-409.